

Molecular Structure of Salt Solutions: A New View of the Interface with Implications for Heterogeneous Atmospheric Chemistry

Pavel Jungwirth^{†,‡} and Douglas J. Tobias^{*,§}

J. Heyrovsky Institute of Physical Chemistry, Academy of Sciences of the Czech Republic, and Center for Complex Molecular Systems and Biomolecules, Dolejskova 3, 18223 Prague 8, Czech Republic, Department of Chemistry, University of Southern California, Los Angeles, California 90089-0482, and Department of Chemistry and Institute for Surface and Interface Science, University of California, Irvine, California 92697-2025

Received: July 17, 2001

Most salts raise the surface tension of water. Interpretation of this phenomenon via the Gibbs adsorption equation has led to the commonly held belief that the ions are repelled from the air/solution interface. Here, we report results from molecular dynamics simulations of a series of sodium halide solution/air interfaces. The simulations reproduce the experimentally measured increases in surface tension relative to pure water. Analysis of the structure reveals that the small, nonpolarizable fluoride anion is excluded from the interface, in accord with the traditional picture. However, all of the larger, polarizable halide anions are present at the interface, and bromide and iodide actually have higher concentrations in the interfacial region than in the bulk. On the basis of the simulations we develop a molecular picture of hydrogen bonding in the interfacial region that might be tested by surface sensitive spectroscopic experiments. The novel, microscopic view of the interfacial structure of aqueous salt solutions presented in this paper has implications for the reactivity of sea salt aerosols in the marine boundary layer, and bromine chemistry in the remote Arctic at polar sunrise.

Heterogeneous chemistry involving sea salt aerosols influences the chemical composition of the atmosphere.^{1–3} Reactions involving halogen anions at the interface between air and the concentrated salt solution comprising the aerosol particles have been proposed to be responsible for the release of reactive halogens into the atmosphere.⁴ However, the presence of ions at the interface is at odds with the prevailing view of the interfacial structure of salt solutions, which is based primarily on surface tension data. It has been known since 1910 that, in aqueous solutions of simple inorganic salts, among which the alkali halides are typical examples, the surface tension increases with solute concentration.⁵ The traditional interpretation of this observation in terms of the Gibbs adsorption equation^{6,7} is that these salts are repelled from the solution/air interface.⁸ Consequently, for many decades the generally accepted notion is that the interface of aqueous electrolyte solutions is devoid of ions, although there have been no direct measurements with molecular resolution to support this view. Here, we demonstrate using molecular dynamics simulations of a series of sodium halide solutions that an increase of surface tension does not necessarily imply negative adsorption of ions. In fact, we show that, whereas the small, nonpolarizable fluoride anion is excluded from the interface, in accord with the traditional picture, all of the larger, polarizable halide anions are present at the interface, and bromide and iodide actually exhibit surfactant activity (enhanced concentration at the interface relative to bulk). The predicted

presence of the heavier halide ions at the solution/air interface provides new insight into the mechanism of chlorine release from sea salt aerosols in the marine boundary layer, and ozone destruction by bromine chemistry in the surface layer at polar sunrise in the Arctic.

We modeled the air/solution interface by performing 1 ns molecular dynamics simulations at 300 K of water slabs containing sodium halide (fluoride, chloride, bromide, or iodide) salts at 1.2 M concentration. For comparison, we carried out a simulation of a slab of pure water. An essential ingredient used in the simulations is a polarizable potential for both water and the ions,^{9,10} which has been shown to be necessary for the proper description of the structure of halogen anion/water clusters.^{11,12} The molecular dynamics simulations were performed using the *Amber6* program package¹³ with polarizable potentials.^{11,14} A slab of 864 water molecules was used to construct each system by adding 18 sodium and 18 halide ions to give a sodium halide concentration of 1.2 M. A simulation of a pure water slab was carried out for comparison with the solution simulations. Each slab was placed into a $30 \times 30 \times 100 \text{ \AA}^3$ rectangular box, and periodic boundary conditions were applied in three dimensions. The simulations were run at a constant temperature of 300 K. The smooth particle mesh Ewald method was used to calculate the electrostatic energies and forces,¹⁵ and the van der Waals interactions and the real space part of the Ewald sum were truncated at 12 Å. A time step of 1 fs was used in the integration of the equations of motion, and the OH bond vibrations were frozen using the SHAKE algorithm.¹⁶ Each simulation consisted of 500 ps equilibration, and 1000 ps data collection.

The surface tensions obtained from the simulations are presented and compared to experimental values in Table 1. In agreement with experimental observations, simulations of all the sodium halide solutions result in a slight increase (less than

* To whom correspondence should be addressed. E-mail: dtobias@uci.edu.

[†] J. Heyrovsky Institute of Physical Chemistry, Academy of Sciences of the Czech Republic, and Center for Complex Molecular Systems and Biomolecules.

[‡] Department of Chemistry, University of Southern California, Los Angeles.

[§] Department of Chemistry and Institute for Surface and Interface Science, University of California.

TABLE 1: Comparison of Simulation and Experimental Results for the Increase in Surface Tension Relative to Pure Water for 1.2 M Aqueous Solutions of Sodium Halide Salts

solution	$\Delta\gamma$ (mN/m) ^a	
	simulation ^b	experiment ^c
NaF	5.1	3.6
NaCl	3.4	2.0
NaBr	2.9	1.6
NaI	2.8	1.2

^a $\Delta\gamma$ is the difference in surface tension between the salt solution and pure water. ^b The surface tension was computed as $\gamma = (1/2)L_z\langle P_{zz} - (P_{xx} + P_{yy})/2 \rangle$, where P_{ii} are the diagonal components of the pressure tensor, L_z is the length of the simulation cell in the direction normal to the interface (z), the angular brackets denote a time average, and the prefactor of $1/2$ accounts for the presence of two interfaces in the slab used for the simulations.³² ^c The experimental values for NaCl, NaBr, and NaI at 1.2 M were obtained by interpolation of data at 1.0 and 1.5 M at 20 °C.³³ The value for NaF was obtained by extrapolation of data from 0 to 0.44 M at 301.6 K.³⁴ Because the concentration dependence of the surface tension increase is highly linear over a wide concentration range (e.g., up to at least 6.0 M for NaCl³³), and the slope does not depend on temperature, our interpolation, extrapolation, and comparison of data at slightly different temperatures are well justified.

10%) of surface tension with respect to pure water, i.e., $\Delta\gamma > 0$. In addition, the simulations correctly reproduce the order of the increase of $\Delta\gamma$, $I^- < Br^- < Cl^- < F^-$. Thus, a key thermodynamic property of the interfaces of alkali halide electrolytes, the moderate increase of surface tension with respect to pure water, is semiquantitatively reproduced by the simulations.

The composite Figure 1 shows typical snapshots from the simulations together with the density profiles within the slab of the ionic species and water oxygen atoms, obtained by averaging over the whole simulation. A striking difference between the small and nonpolarizable sodium cation and fluoride anion on one hand, and all of the heavier halogen anions on the other hand, is immediately evident in the snapshots. In the NaF solution, both ions are strongly repelled from the surface, leaving an ion-free layer roughly 3.5 Å thick (i.e., approximately the diameter of one water molecule). This is in accord with the classical Onsager–Samaras¹⁷ model, in which ions are repelled from the air/water interface by their image charges on the air side. In contrast, Cl^- and especially Br^- and I^- occupy a significant portion of the air/water interface. Quantitatively, this effect is illustrated by the density profiles in Figure 1, and by the relative concentrations of ions in the surface layer, reported in Table 2. Although in the NaF electrolyte the fluoride concentration in the surface layer is reduced by 93% with respect to the bulk, in NaCl solution the chloride concentration drops by only 29%. However, in the NaBr and NaI electrolytes the concentration of anions at the interface is actually enhanced with respect to the bulk, by a factor of 2.1 or 2.9, respectively. Note also, that the heavier halide anions drag a certain fraction of sodium cations to the interface. Nevertheless, the anion concentration at the interface is much higher than the cation concentration, whereas just below the surface layer the relative abundance of anions and cations is reversed, resulting in the creation of an electrical double layer (Figure 1). The propensity of large, polarizable anions for the interface can be rationalized qualitatively in terms of anisotropic solvation, which induces a substantial dipole on the ion.¹² The resulting favorable dipole–dipole interactions compensate the loss of ion–dipole interactions that accompanies the transfer of an ion from the bulk solution to the interface.

There are several independent experimental observations that are consistent with our predictions of the relative preferences

of halide anions for the air/water interface. Perhaps the most relevant are measurements of differences in surface potentials, $\Delta\chi$, between ionic solutions and pure water.¹⁸ A positive $\Delta\chi$ was measured for KI, KBr, and KCl solutions, and this has been suggested to imply an ionic double layer near the surface, with its positive side directed into the bulk solution.¹⁸ Our simulations confirm this hypothesis. Moreover, our prediction of an increase in anion adsorption in the order $I^- > Br^- > Cl^-$ is consistent with the observed order of $\Delta\chi$ values ($KI > KBr > KCl \approx 0$). The small, negative value of $\Delta\chi$ measured for KF is in accord with the slightly greater repulsion of F^- vs Na^+ from the interface in our simulation of the NaF solution (Figure 1). Using X-ray photoelectron spectroscopy and scanning electron microscopy, Ghosal et al. directly observed selective segregation of Br^- to the surface of bromide doped NaCl crystals under conditions of relative humidity where partial dissolution of the surface takes place.¹⁹ Indirect evidence for the presence of chloride and bromide ions at aqueous interfaces includes the enhanced reactive uptake of molecular halogens by the surfaces of halide solutions.²⁰ Recent measurements of the kinetics of chlorine production by photochemically induced reactions of ozone with sea salt aerosols could not be explained by bulk phase chemistry involving chloride anions. However, a mechanism involving chloride anions at the aerosol solution/air interface was found to quantitatively reproduce the measured kinetics.⁴ The presence of the larger, polarizable anions at the bulk solution/air interface is also consistent with a large number of experimental and theoretical observations of surface locations of these ions on small to moderately sized water clusters^{10,12,21–25}. This suggests that the essential features of interfacial solvation inferred from cluster studies may indeed be extrapolated to the bulk solution interface.

We have used the simulations to develop a microscopic description of water–water and anion–water hydrogen bonding in the interfacial region of the electrolyte solutions that might be tested by surface sensitive spectroscopic techniques. To this end, we define a vector pointing from the oxygen atom of a water molecule acting as a hydrogen bond donor to the atom acting as a hydrogen bond acceptor, i.e. a water oxygen or anion (Figure 2a). In Figure 2, we show distributions of the cosine of the angle between these vectors and a vector normal to the interface. Figure 2b contains the results for water–water hydrogen bonds in the interfacial region. All of the interfaces show a similar hydrogen bond orientational distribution, with a maximum at $\cos(\theta_{ww}) \approx 0$, indicating a strong preference for water–water hydrogen bonds parallel to the interface. The distribution for the NaF solution is identical to that of pure water, whereas those for the other electrolyte solutions show subtle differences. In particular, the distribution is progressively shifted toward $\cos(\theta_{ww}) > 0$ as the anion is changed in the order Cl^- , Br^- , I^- . This implies a small increase of water–water hydrogen bonds perpendicular to the interface at the expense of hydrogen bonds parallel to the interface. The relatively minor modification of the water–water hydrogen bonding observed here is consistent with the only slight alteration by 0.6 M NaCl of the interfacial water structure detected in a recent vibrational sum frequency generation experiment.²⁶

In contrast to the weak dependence of the interfacial water–water hydrogen bond orientational distributions on the identity of the halide ion, that of the corresponding anion–water distributions is dramatic (Figure 2c). The distribution for F^- is strongly peaked at $\cos(\theta_{wx}) = -1$, indicating a predominance of water–anion hydrogen bonds pointing toward the interior of the solution. This is completely consistent with the classical

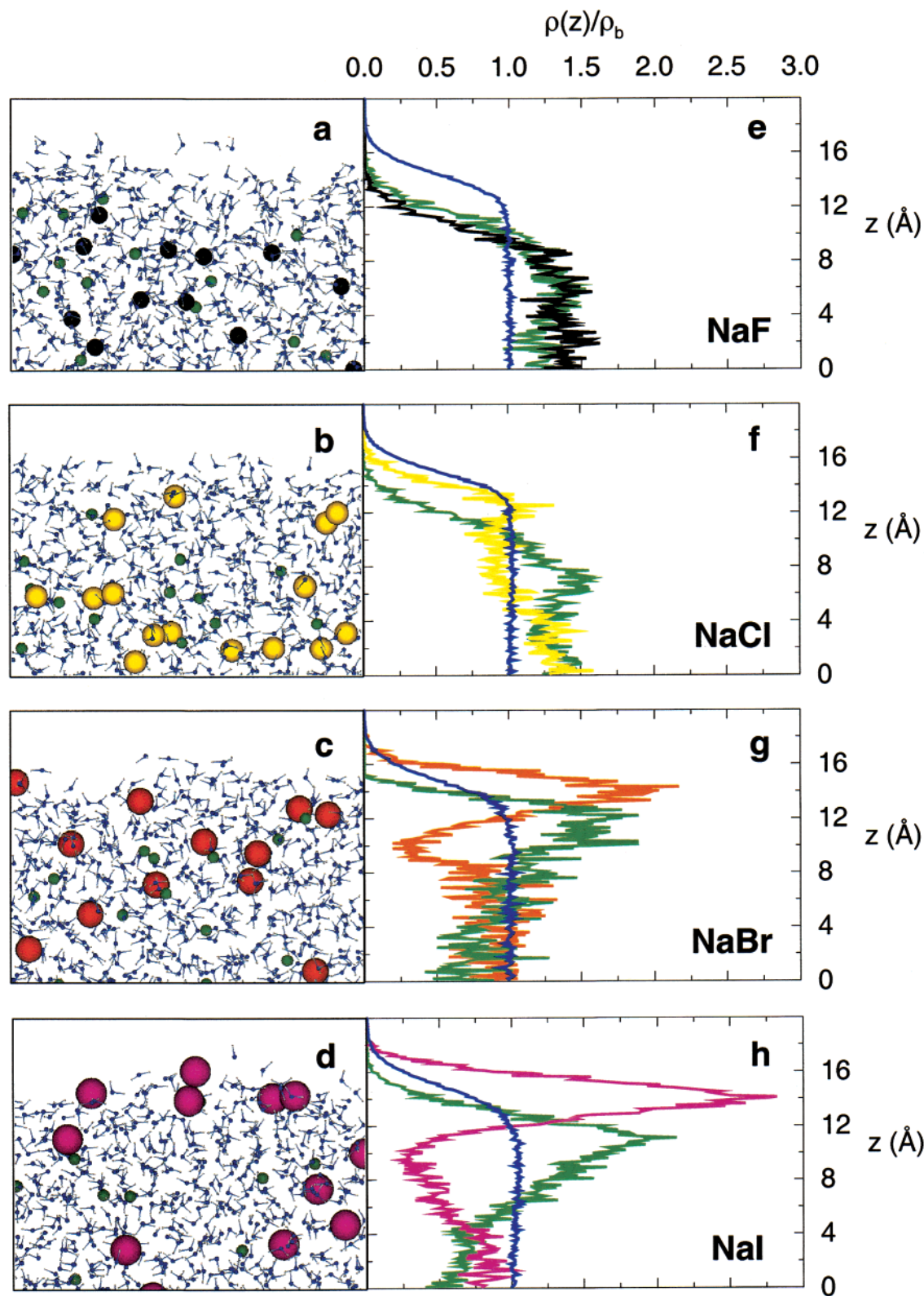


Figure 1. a–d, Snapshots of the solution/air interfaces from the molecular dynamics simulations. Coloring scheme: water oxygen, blue; water hydrogen, gray; sodium ions, green; chloride ions, yellow; bromide ions, orange; iodide ions, magenta. e–h, Number densities, $\rho(z)$, of water oxygen atoms and ions plotted vs distance from the center of the slabs in the direction normal to the interface (z), normalized by the bulk water density, ρ_b . The ion densities have been scaled by the water/ion concentration ratio of 48 for ease of comparison. The colors of the curves correspond to the coloring of the atoms in the snapshots.

notion of an ion-depleted interface with a subsurface layer of ions. In this situation, the only way for water molecules at the interface to make hydrogen bonds with the anions is by pointing an OH bond toward the bulk. In the case of the NaBr and NaI

solutions, where the anions preferentially adsorb to the interface, the ion–water hydrogen bonds are preferentially aligned nearly parallel to the interface, with a peak in the distribution at $\cos(\theta_{wx}) \approx 0.2$. In the NaCl solution, where the anion concentration

TABLE 2: Interfacial Concentrations of Ions from Simulations of 1.2 M Sodium Halide Solutions

solution	relative concentration ^a	
	Na ⁺	X ⁻
NaF	0.16	0.07
NaCl	0.16	0.71
NaBr	0.81	2.10
NaI	0.69	2.91

^a Ratio of the concentration of ions in the interface (defined as $|z| > 12.5$ Å, which is where the oxygen density begins to deviate from its bulk value) to the concentration in the whole system.

at the interface is neither significantly enhanced nor depleted with respect to the bulk, the ion–water hydrogen bond orientational distribution accordingly appears intermediate between the F⁻ (depleted) and Br⁻/I⁻ (enhanced) cases.

It should be possible to detect the differences in water–anion hydrogen bonding predicted by our simulations with a surface sensitive vibrational spectroscopic technique, such as sum frequency spectroscopy, which was used very recently to probe differences in hydrogen bonding between air/water and nonpolar liquid/water interfaces.²⁷ Water–halide hydrogen bonds are stronger than water–water hydrogen bonds,²⁸ and hence the stretching of an OH bond participating in a water–halide hydrogen bond occurs at a lower frequency than in a water–water hydrogen bond.²³ We have computed the average number of water–halide hydrogen bonds per water molecule in the interfacial region, obtaining 0.02 for F⁻, 0.07 for Cl⁻, 0.13 for Br⁻, and 0.17 for I⁻. Thus, we predict that there should be an increasing amount of red-shifted intensity in the OH stretching region for interfacial water moving in the series F⁻, Cl⁻, Br⁻, I⁻. Moreover, a polarized measurement might be able to detect differences between the NaF solution, where the water–anion bonds are preferentially oriented perpendicular to the interface, the NaBr and NaI solutions, where they are preferentially oriented parallel to the interface, and the intermediate NaCl solution.

The present study sheds new light on the structure of the air/water interface of electrolyte solutions. Historically, simple electrolyte solutions have been regarded as having an interfacial layer devoid of ions. We have verified that this is the case for aqueous NaF, where both the anion and cation are small and relatively nonpolarizable. However, we have clearly demonstrated in the present study that the structure of the interface can be altered drastically by the particular choice of the dissolved salt. Specifically, for the series of sodium halides, upon moving from fluoride to the larger, more polarizable halides, the interfacial region becomes increasingly populated by ions. Ultimately, for bromide and iodide there is actually an enhancement of the anionic concentration at the interface relative to the bulk. For these systems, it is misleading to use the Gibbs equation, derived from the thermodynamics of the interface, to infer the molecular structure.

The predicted surface enhancement of heavier halides in alkali halide solutions is not only interesting from the point of view of standard theories of adsorption phenomena, but it has also direct relevance to atmospheric chemistry. Reactions involving halide ions at the air/water interface have been implicated in the release of reactive halogens into the atmosphere.⁴ In recent years, the important role of aqueous sea-salt aerosols in the chemistry of the marine boundary layer has been firmly established.^{1–3} A particularly intriguing observation is that bromine chemistry is enhanced relative to that expected from the 1:650 molar ratio of Br⁻:Cl⁻ in sea salt. For example, ozone destruction in the surface layer at polar sunrise in the Arctic

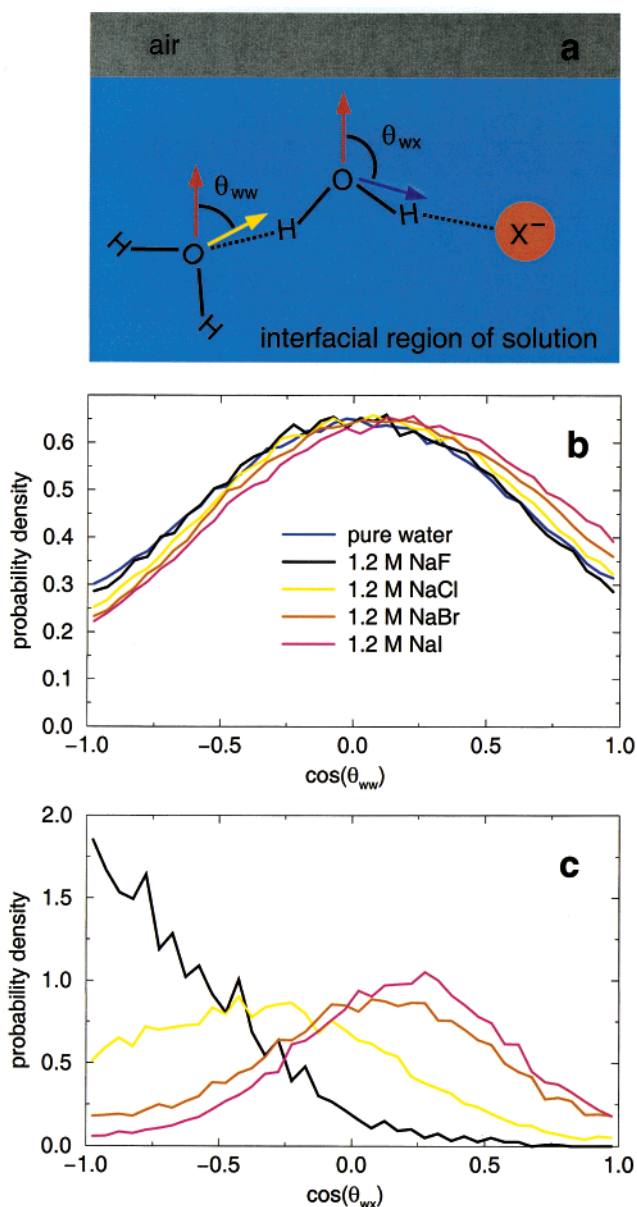


Figure 2. Distribution of the orientations of hydrogen bonds in the interfacial region ($|z| > 12.5$ Å). **a**, Definition of the hydrogen bond orientation: θ_{ww} is the angle between a vector (yellow arrow) pointing from one oxygen to the other in a hydrogen bonded pair of water molecules and a vector normal to the interface (red arrow); θ_{wx} is the analogous angle for a vector (blue arrow) defining the direction of a water–anion hydrogen bond. A water molecule is considered hydrogen bonded to a hydrogen bond acceptor, A, if the O–A distance is less than a cutoff value (3.5 Å for water–water, 3.3 Å for fluoride–water, 3.7 Å for chloride–water, 4.1 Å for bromide–water, and 4.3 Å for iodide–water), and the angle between the O–A axis and one of the O–H bonds is less than 30°. **b**, Distribution of water–water hydrogen bond orientations. **c**, Distribution of halide anion–water hydrogen bond orientations.

was initially attributed to bromine chemistry,²⁹ and recently confirmed by measurements of Br₂ and BrCl in air during ozone depletion episodes.³⁰ Although there are several mechanisms that could lead to the enhancement of bromine compared to chlorine when sea salt freezes on the snowpack,³¹ the results of the present study suggest that the intrinsic propensity of bromine for the air/solution interface is an important factor. The present study also suggests that interfacial phenomena will play an even more important role in iodide chemistry.

Acknowledgment. We thank Stephen Bradforth, Barbara Finlayson-Pitts, John Hemminger, and Reg Penner for valuable discussions and comments on the manuscript. Support to P. J. from the U. S. Department of Energy and the Czech Ministry of Education (LN00A032), and to D. T. from the U. S. National Science Foundation (MCB-0078278), is gratefully acknowledged. P. J. is a recipient of a NATO Science Senior Fellowship.

References and Notes

- (1) Ravishankara, A. R. *Science* **1997**, 276, 1058–1065.
- (2) Andreae, M. O.; Crutzen, P. J. *Science* **1997**, 276, 1052–1058.
- (3) Finlayson-Pitts, B. J.; Hemminger, J. C. *J. Phys. Chem. A* **2000**, 104, 11 463–11 477.
- (4) Knipping, E.; Lakin, M. J.; Foster, K. L.; Jungwirth, P.; Tobias, D. J.; Gerber, R. B.; Dabdub, D.; Finlayson-Pitts, B. J. *Science* **2000**, 288, 301–306.
- (5) Heydweiller, A. *Ann. Physik. (4)* **1910**, 33, 145.
- (6) Gibbs, J. W. *The Collected Works of J. Willard Gibbs*; Longmans: New York, 1928.
- (7) Chattoraj, D. K.; Birdi, K. S. *Adsorption and the Gibbs Surface Excess*; Plenum: New York, 1984.
- (8) Adam, N. K. *The Physics and Chemistry of Surfaces*; Oxford University Press: London, 1941.
- (9) Caldwell, J.; Dang, L. X.; Kollman, P. A. *J. Am. Chem. Soc.* **1990**, 112, 9144–9147.
- (10) Perera, L.; Berkowitz, M. L. *J. Chem. Phys.* **1991**, 95, 1954–1963.
- (11) Perera, L.; Berkowitz, M. L. *J. Chem. Phys.* **1994**, 100, 3085–3093.
- (12) Tobias, D. J.; Jungwirth, P.; Parrinello, M. *J. Chem. Phys.* **2001**, 114, 7036–7044.
- (13) Case, D. A.; Pearlman, D. A.; Caldwell, J. W.; Cheatham III, T. E.; Ross, W. S.; Simmerling, C. L.; Darden, T. A.; Merz, K. M.; Stanton, R. V.; Cheng, A. L.; Vincent, J. J.; Crowley, M.; Tsui, V.; Radmer, R. J.; Duan, Y.; Pitera, J.; Massova, I.; Seibel, G. L.; Singh, U. C. *AMBER6*; University of California: San Francisco, 1999.
- (14) Markovich, G.; Perera, L.; Berkowitz, M. L.; Cheshnovsky, O. *J. Chem. Phys.* **1996**, 105, 2675–2685.
- (15) Essmann, U.; Perera, L.; Berkowitz, M. L.; Darden, T.; Pedersen, L. G. *J. Chem. Phys.* **1995**, 103, 8577–8593.
- (16) Ryckaert, J.-P.; Ciccotti, G.; Berendsen, H. J. C. *J. Comput. Phys.* **1977**, 23, 327–341.
- (17) Onsager, L.; Samaras, N. N. T. *J. Chem. Phys.* **1934**, 2, 528–536.
- (18) Randalls, J. E. B. *Phys. Chem. Liq.* **1977**, 7, 107–179.
- (19) Ghosal, S.; Shbeeb, A.; Hemminger, J. C. *Geophys. Res. Lett.* **2000**, 27, 1879–1882.
- (20) Hu, J. H.; Shi, Q.; Davidovits, P.; Worsnop, D. R.; Zahniser, M. S.; Kolb, C. E. *J. Phys. Chem.* **1995**, 99, 8768–8776.
- (21) Dang, L. X.; Smith, D. E. *J. Chem. Phys.* **1993**, 99, 6950–6956.
- (22) Markovich, G.; Pollack, S.; Giniger, R.; Cheshnovsky, O. *J. Chem. Phys.* **1994**, 101, 9344–9353.
- (23) Ayotte, P.; Weddle, G. H.; Kim, J.; Johnson, M. A. *J. Am. Chem. Soc.* **1998**, 120, 12361–12362.
- (24) Stuart, S. J.; Berne, B. J. *J. Phys. Chem. A* **1999**, 103, 10 300–10 307.
- (25) Gora, R. W.; Roszak, S.; Leszczynski, J. *Chem. Phys. Lett.* **2000**, 325, 7–14.
- (26) Schnitzer, C.; Baldelli, S.; Shultz, M. J. *J. Phys. Chem. B* **2000**, 104, 585–590.
- (27) Scatena, L. F.; Brown, M. G.; Richmond, G. L. *Science* **2001**, 292, 908–912.
- (28) Arshadi, M.; Yamdagni, R.; Kebarle, P. *J. Phys. Chem.* **1970**, 74, 1475–1482.
- (29) Barrie, L. A.; Bottenheim, J. W.; Schnell, R. C.; Crutzen, P. J.; Rasmussen, R. A. *Nature* **1988**, 334, 138.
- (30) Foster, K. L.; Plastring, R. A.; Bottenheim, J. W.; Shepson, P. B.; Finlayson-Pitts, B. J.; Spicer, C. W. *Science* **2001**, 291, 471–474.
- (31) Koop, T.; Kapilashrami, A.; Molina, L. T.; Molina, M. J. *J. Geophys. Res.* **2000**, 105, 26 393–26 402.
- (32) Zhang, Y.; Feller, S. E.; Brooks, B. R.; Pastor, R. W. *J. Chem. Phys.* **1995**, 103, 10 252–10 266.
- (33) Washburn, E. W. *International Critical Tables of Numerical Data, Physics, Chemistry, and Technology*; McGraw-Hill: New York, 1928; Vol. IV.
- (34) Hey, M. J.; Shield, D. W.; Speight, J. M.; Will, M. C. *J. Chem. Soc., Faraday Trans. 1* **1981**, 77, 123–128.